

## Emission of Electromagnetic Pulses from Laser Wakefields through Linear Mode Conversion

Zheng-Ming Sheng,<sup>1,2</sup> Kunioki Mima,<sup>2</sup> Jie Zhang,<sup>1</sup> and Heiji Sanuki<sup>3</sup>

<sup>1</sup>Laboratory of Optical Physics, Institute of Physics, CAS, Beijing 100080, China

<sup>2</sup>Institute of Laser Engineering, Osaka University, Suita, Osaka 565-0871, Japan

<sup>3</sup>National Institute for Fusion Science, Toki, Gifu 509-5292, Japan

(Received 26 August 2004; published 9 March 2005)

Powerful coherent emission around the plasma oscillation frequency can be produced from a laser wakefield through linear mode conversion. This occurs when the laser pulse is incident obliquely to the density gradient of inhomogeneous plasmas. The emission spectrum and conversion efficiency are obtained analytically, which are in agreement with particle-in-cell simulations. The emission can be tuned to be a radiation source in the terahertz region and with field strengths as large as a few GV/m, suitable for high-field applications. The emission also provides a simple way to measure the wakefield produced for particle acceleration.

DOI: 10.1103/PhysRevLett.94.095003

PACS numbers: 52.25.Os, 52.35.Mw, 52.59.Ye

A laser wakefield is an electron plasma wave driven by the ponderomotive force of a laser pulse [1]. It has been studied intensively for the purpose of particle acceleration [2,3]. Alternatively, it can be used for photon acceleration or frequency up-conversion of a laser pulse [4], laser pulse compression [5], and more recently light intensification [6]. Since the typical plasma oscillation frequency for these applications is in the terahertz (THz) range, the wakefield can potentially serve as a powerful THz emitter [7]. Currently, it is still challenging to obtain intense THz emission for various applications [8]. On the other hand, even though the laser wakefield can be driven at high amplitudes, usually a plasma wave cannot convert into an electromagnetic wave directly because of their different dispersion relations. Recently, it has been found from numerical simulations that intense radiation around the plasma frequency can be produced from the wakefield in inhomogeneous plasma [9], whereas the mechanism involved remains unsolved.

In this Letter, we propose that a laser wakefield can emit intense low-frequency radiation around the plasma frequency through linear mode conversion. It is well known that an electromagnetic wave can convert into an electrostatic wave through linear mode conversion, which leads to the resonance absorption of light in inhomogeneous plasmas [10]. Means *et al.* studied the inverse problem and found that there is a reversal symmetry in the electromagnetic-electrostatic mode conversion [11], which was confirmed later by Hinkel-Lipsker *et al.* [12]. Similarly, we find that linear mode conversion from the laser wakefield to electromagnetic pulses can occur in certain conditions as explained below. It can explain our earlier simulation results [9] as well as even earlier experimental observations [7]. Since the wakefield can be excited at amplitudes as high as 100 GV/m even at the plasma density  $10^{18} \text{ cm}^{-3}$  (at which the plasma frequency  $\omega_p/2\pi = 9 \text{ THz}$ ) [3], the field strength of the mode-converted emission can reach a few GV/m, which is still difficult to achieve by other known methods [8].

Let us consider the laser wakefield excitation when a plane laser pulse propagates at an angle of  $\theta$  to the density gradient of an inhomogeneous plasma slab, as shown in Fig. 1. The plasma slab is underdense with a trapezoid density profile along the  $x$  direction. To describe the problem, a simple way is to transform all variables into a moving frame  $V = c \sin\theta \mathbf{e}_y$ , where  $\mathbf{e}_y$  is a unit vector along the  $y$  direction. In this frame, one can derive a set of equations for the electron momentum, electron density, and scalar and vector potentials for the wakefield and its emission, which are the same as those given by Lichters *et al.* [13] for laser-solid interactions. Here we give only the equation for the vector potential associated with the wakefield emission as follows:

$$\left( \frac{\partial^2}{\partial x^2} - \frac{\partial^2}{\partial t^2} - \frac{n}{\gamma \cos\theta} \right) \mathbf{a} = \mathbf{e}_y \left[ \Theta(x) - \frac{n}{\gamma \cos\theta} \right] \tan\theta, \quad (1)$$

where  $\mathbf{a}$  is normalized by  $mc^2/e$ , the electron density  $n$  by  $n_0/\cos\theta$ ,  $x$  and  $t$  by  $c/\omega_{p0}$  and  $\omega_{p0}^{-1}$ , respectively,  $\omega_{p0} = (4\pi n_0 e^2/m)^{1/2}$ ,  $\lambda_{p0} = 2\pi c/\omega_{p0}$ ,  $\gamma$  is the relativistic factor, and the unperturbed electron density  $n_{0e}(x) = n_0 \Theta(x)$ , which is in arbitrary profiles. Equation (1) suggests there exists emission from the wakefield around the plasma

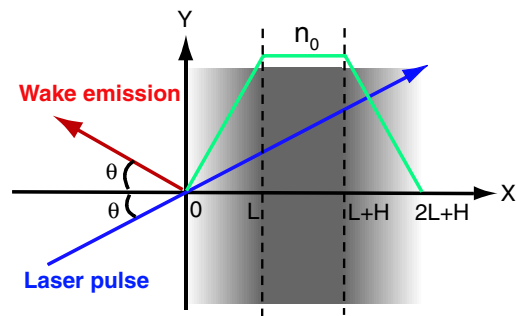


FIG. 1 (color online). Schematic of electromagnetic emission from a wakefield generated by a laser pulse incident obliquely to the plasma density gradient.

frequency if  $\theta \neq 0$ . The emission is always  $p$  polarized with the emitting angle of  $\theta$ . However, since the electrostatic and electromagnetic waves have different dispersion relations, it is usually difficult to fulfill the phase match conditions, which is necessary to have a high conversion efficiency.

To seek plasma conditions to fulfill the phase match, let us consider the evolution of a laser wakefield in nonuniform tenuous plasma, where the laser pulse propagates nearly with the vacuum speed of light. In the moving frame mentioned above, the frequency and wave numbers of the incident laser pulse are given by  $(\omega, k_x, k_y, k_z) = (\omega_0 \cos\theta, k_0 \cos\theta, 0, 0)$  by use of the Lorentz transform, where  $\omega_0$  and  $k_0$  are, respectively, the laser frequency and wave number in the laboratory frame. Therefore the laser pulse is a function of  $(t - x)\cos\theta$  in the moving frame, and the displacements of electrons at initial positions  $x_0$  in the driven laser wakefield should follow as  $\delta(x_0, t) = \delta_0 \cos[\psi(x_0, t)]$ , where  $\psi(x_0, t) = \omega_p(x_0) \times (t - x_0)\cos\theta$ . For this wakefield, its local wave vector, defined by  $k = -\partial\psi/\partial x_0$ , changes with time and space. If the plasma density rises linearly as  $n_{0e} = n_0(x/L)$ , one finds the wave vector

$$k(x_0, t) = \omega_p(x_0)(3x_0 - t)\cos\theta/2x_0. \quad (2)$$

It suggests that  $k(x_0, t) = 0$  along the line  $x_0 = t/3$ . Note that longitudinal and transverse waves in plasma can couple efficiently in linear approximation only at  $k = 0$  and  $\omega = \omega_p$ , where their dispersion curves meet. In the present case, the mode conversion from electrostatic to electromagnetic waves becomes possible along the line  $x_0 = t/3$ . The phase velocity, which evolves as  $v_{\text{ph}}(x_0, t) = \omega/k = -(\partial\psi/\partial t)/(\partial\psi/\partial x_0) = 2x_0/(3x_0 - t)$ , changes its sign around the same straight line. On the other hand, if the plasma density declines as  $n_{0e} = n_0(1 - x/L)$  for  $0 \leq x \leq L$ , the wave vector changes as

$$k(x_0, t) = \omega_p(x_0)(2L + t - 3x_0)\cos\theta/[2(L - x_0)]. \quad (3)$$

It indicates that there are always  $k > 0$  and  $v_{\text{ph}} > 0$  since there is  $t \geq x_0$  in the wakefield. This implies that the linear mode conversion from electrostatic to electromagnetic waves does not occur.

To check the validity of above analysis, we conduct a series of one-dimensional particle-in-cell (1D PIC) simulations. Our code adopts a boosted frame moving along  $y$  direction in order to deal with the oblique incidence of the laser pulse as in Ref. [13]. The laser pulse has a sine-square profile  $a_L = a_0 \sin^2[\pi(x - ct)/d_L]$  for  $0 \leq (x - ct) \leq d_L$ , which enters the left boundary of the simulation box with  $s$  polarization in order to distinguish it easily from the  $p$  polarized emission from the wakefield. We take  $a_0 = 0.5$  and  $d_L = 20\lambda_0$ , with  $\lambda_0$  the laser wavelength in vacuum. Figure 2 shows the longitudinal and transverse fields in the  $x - t$  plane. In the inhomogeneous regions, Fig. 2(a) shows that the phase velocity of the wakefield changes with time. In particular, the phase velocity changes its sign in the re-

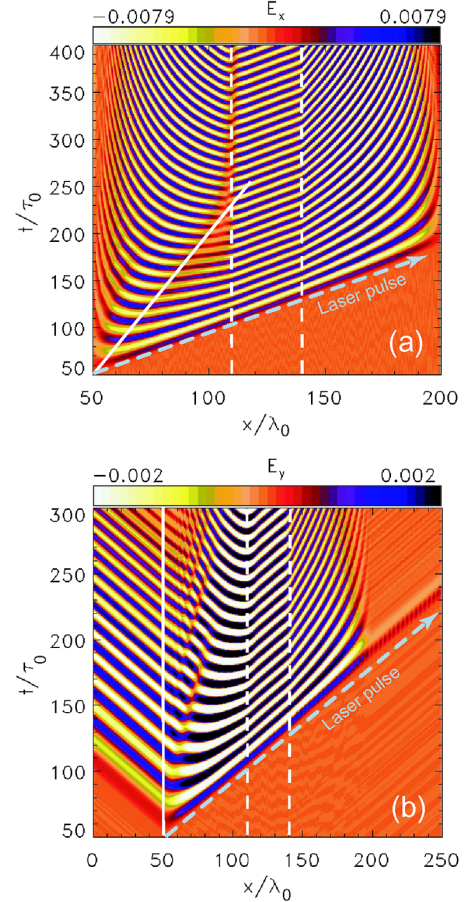


FIG. 2 (color online). Spatial-temporal plots of the longitudinal field (a) and transverse field (b) from 1D PIC simulation. The pulse is with  $a_0 = 0.5$ ,  $d_L = 20\lambda_0$ , and  $\theta = 25^\circ$ , and the plasma with  $L = 60\lambda_0$  and  $n_0/n_c = 0.01$ . The plasma density rises linearly from  $x = 50\lambda_0$  until  $110\lambda_0$ , and declines linearly from  $x = 140\lambda_0$ . It is homogeneous at  $n_0$  within the dashed lines. The solid line in (a) shows  $x = t/3$  and that in (b) shows the vacuum-plasma boundary. The laser pulse runs along  $x = t$  at the lower edge of the structure having the temporal width of nearly one plasma oscillation, and it is not visible because of  $s$  polarization. The fields are normalized by  $m\omega_0 c/e$  and  $\tau_0 = 2\pi/\omega_0$ .

gion with increasing densities (between  $x = 50\lambda_0$  and  $110\lambda_0$ ) along the line  $x = t/3$ , as described by Eq. (2). Around this line, mode conversion from the wakefield to electromagnetic emission occurs. The reduced field amplitude inside plasma along the line  $x = t/3$  indicates that a significant part of electrostatic energy is converted into electromagnetic energy, which propagates away. Figure 2(b) plots the transverse field component. In addition to the fields inside plasma (due to the oblique incidence of the laser pulse), there are also fields across the left vacuum-plasma boundary in the vacuum region ( $x < 50\lambda_0$ ). This is just due to the wakefield emission through linear mode conversion. On the other hand, in the region with declining densities (between  $x = 140\lambda_0$  and  $200\lambda_0$ ), the phase velocity decreases with time but never changes its sign as described by Eq. (3). As a result, there is almost no electromagnetic emission across the rear side of the

plasma-vacuum interface at  $x = 200\lambda_0$ . In the region with a homogeneous plasma density between  $x = 110\lambda_0$  and  $140\lambda_0$ , the phase velocity does not change with time and space.

An important factor is the conversion efficiency, which depends upon the plasma density gradient, the incident angle, and the laser parameters. It has been shown that the problem of mode conversion from electrostatic to electromagnetic waves is symmetric with its inverse problem [11,12]. Therefore, we take a simple mode conversion efficiency for cold plasma [14]:

$$\eta = 2\alpha q(2 + \alpha q)^{-1} \exp(-4q^{3/2}/3), \quad (4)$$

where  $\alpha = 4\pi^2[Ai'(0)]^2 = 2.644$  and  $q = (\omega L_\omega/c)^{2/3} \times \sin^2\theta$ , which depends on the emission frequency  $\omega$ , the corresponding plasma scale length  $L_\omega$ , and the incident angle  $\theta$ . For a plasma density  $n_{0e} = n_0(x/L)$ ,  $L_\omega = L(\omega_p/\omega_{p0})^2 = L(\omega/\omega_{p0})^2$ . Let  $\tilde{\omega} = \omega/\omega_{p0}$ , then  $q = (\omega_{p0}L/c)^{2/3} \tilde{\omega}^2 \sin^2\theta$ . Since the maximum conversion efficiency (about 0.5) is found at  $q = 0.46$ , the emission peak occurs at the frequency  $\tilde{\omega} \approx 0.68(\omega_{p0}L/c)^{-1/3}(\sin\theta)^{-1}$ , if ignoring the different wakefield amplitudes excited at different positions. In our case, the mode conversion sweeps across the inhomogeneous region with increasing densities (or frequencies) along the line  $x = t/3$ . Accounting for different wake amplitudes at different positions, the emission spectrum can be written as

$$S(\tilde{\omega}, L, \theta, d_L) = \eta[q(\tilde{\omega})]E_m^2(\tilde{\omega}), \quad (5)$$

where  $E_m$  is the wakefield amplitude for the local frequency  $\tilde{\omega}$  at  $x = L\tilde{\omega}^2$ . If the plasma density is weakly inhomogeneous, the local wakefield amplitude can be approximated by a corresponding value in homogeneous plasma. For a sine-square pulse profile  $a_L = a_0 \sin^2[\pi(x - ct)/d_L]$ , for example, the wakefield amplitude at a given plasma density (corresponding to  $\omega_p$ ) is given by  $E_m(\omega_p) = (m\omega_p c/e)(a_0^2/4) \sin(\pi d_L/\lambda_p) \times \{[1 - (d_L/\lambda_p)^2]^{-1} - 0.25[1 - 0.25(d_L/\lambda_p)^2]^{-1}\}$  [3,5]. Now, for the given linear density profile, substituting  $\omega_p$  with  $\omega$  and  $d_L/\lambda_p = (\omega d_L/2\pi c) = \tilde{\omega}(d_L/\lambda_{p0})$  into  $E_m$  given above, one obtains the emission spectrum with Eq. (5). Figure 3(a) plots the emission spectrum for different incident angles at the fixed  $L = 6\lambda_{p0}$  and  $d_L = 2\lambda_{p0}$ . The optimal angle of incidence is around  $\theta = 15^\circ$ , where the spectrum is peaked around frequency  $\tilde{\omega} \approx 0.75$ . At larger angles of incidence, the spectrum peaks are shifted to lower frequencies and the spectrum widths reduce. Note that there is no emission at  $\theta = 0^\circ$ . Figure 3(b) shows the emission spectrum at different density scale lengths  $L$ . It depends weakly on  $L$ . This reminds us that the pulse duration  $d_L$  is a key parameter to control the central frequency  $\omega_c$  of the spectrum. One can tune the spectrum by changing  $\omega_{p0}$  (or  $\lambda_{p0}$ ) and  $d_L$ . If  $d_L/\lambda_{p0}$  is fixed, the spectrum profile (together with its magnitude)  $S(\omega/\omega_{p0})(a_0^2\omega_{p0})^{-2}$  is fixed for given  $L$  and  $\theta$ .

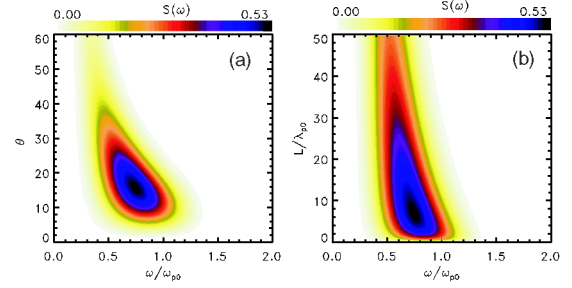


FIG. 3 (color online). (a) Emission spectra based on Eq. (5) as a function of the incident angles of the laser pulse for a plasma density scale length  $L = 6\lambda_{p0}$ . (b) Emission spectra as a function of the density scale length for the incident angle of  $15^\circ$ . The incident pulse is with a sine-square profile for  $d_L = 2\lambda_{p0}$ .

To check the reliability of the present model, we compare the spectra predicted by the model with the simulation results. Figure 4(a) displays the emitted pulses for three different angles of incidence at the laser amplitude  $a_0 = 0.5$ . The peak amplitude for the incident angle of  $15^\circ$  is over  $0.002m\omega_0 c/e$ . The corresponding field strength is about 6.4 GV/m and its intensity about  $5.48 \times 10^{12}$  W/cm<sup>2</sup> for  $\lambda_0 = 2\pi c/\omega_0 = 1 \mu\text{m}$ . One notes that the emitted pulses are all with frequency chirp. This is because the linear mode conversion sweeps across the inhomogeneous plasma from low to high densities. Their temporal profiles are determined by the local wakefield amplitudes excited, the incident angles, and plasma density gradients according to Eq. (5). Qualitatively, for the spatial distributions of the wakefield amplitude  $E_m(x/L_\omega)$  and conversion efficiency  $\eta(x/L_\omega)$  in the inhomogeneous plasma, the temporal profiles of the emitted pulses appear as  $\eta^{1/2}(\omega t)E_m(\omega t)$  with  $\omega = \omega_p(x)$ . Figure 4(b) illustrates the corresponding spectra both from the model calculation and the PIC simulations. They agree each other very well not only in the spectrum profiles, but also in the relative intensities. In passing, the chirped pulses may be further compressed to shorter durations and higher amplitudes by propagating through another plasma slab, which exhibits anomalous dispersion.

Equation (5) suggests that the emission scales proportional to  $a_0^4$ . Figure 4(c) plots the emission spectra at different laser intensities. It agrees with Eq. (5) very well for  $a_0 < 1$ . At higher intensities, the spectrum peaks are lower than the  $a_0^4$  scaling because the wakefield amplitude  $E_m$  is no longer proportional to  $a_0^2$ . Meanwhile, at very high intensities, plasma wave breaking occurs. This results in a complicated spectrum structure, as shown by the curve for  $a_0 = 3$ .

The energy conversion efficiency is obtained by integrating the mode-converted energy divided by the laser energy. It is given by

$$\eta_E = \frac{a_0^2}{2} \frac{L}{g(d_L)} \frac{\omega_{p0}^2}{\omega_0^2} \int_0^\infty \eta[q(\tilde{\omega})]E_m^2\left(\tilde{\omega}, \frac{d_L}{\lambda_{p0}}\right) \tilde{\omega} d\tilde{\omega}, \quad (6)$$

where  $g(d_L)$  is the spatial integral over the pulse profile and

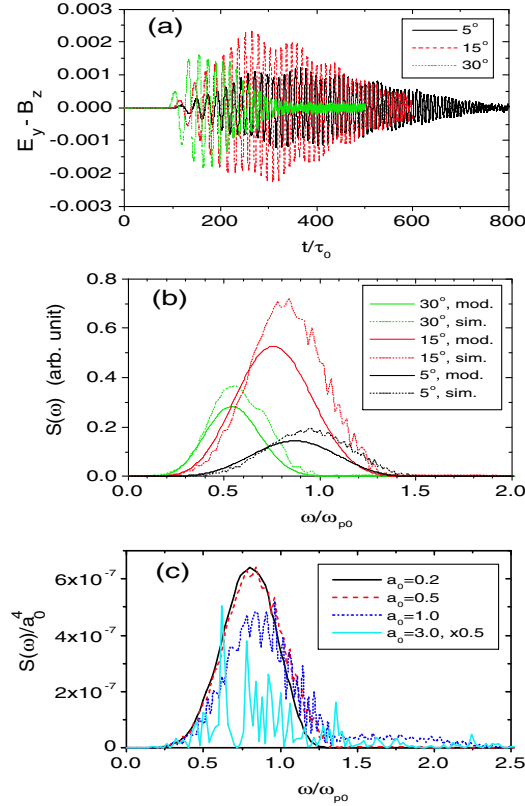


FIG. 4 (color online). (a) Time dependence of the emission at different incident angles for the laser pulse with  $a_0 = 0.5$  and  $d_L = 20\lambda_0$  and the plasma with  $L = 60\lambda_0$  and  $n_0/n_c = 0.01$ . The field is normalized by  $m\omega_0 c/e$ . (b) Comparison of emission spectra between the model calculation and PIC simulations. The simulation results have been multiplied by the same factor. (c) Emission spectra from PIC simulations for different laser intensities. The spectra have been divided by  $a_0^4$ , and the spectrum for  $a_0 = 3.0$  has been multiplied by an additional factor of 0.5.

$\tilde{E}_m(\tilde{\omega}, d_L/\lambda_{p0})$  is the wakefield amplitude normalized by  $(a_0^2/2)m\omega_{p0}c/e$ . The integral depends upon  $L$ ,  $\theta$ , and the pulse profile. Note that  $\eta_E \propto a_0^2$ . For simulation parameters given in Fig. 4(a) and around the optimized angles of incidence about  $10^\circ$ – $15^\circ$ , one finds  $\eta_E \approx 0.0005$ . This agrees with the numerical simulations given in Fig. 4(a) for the incident angle of  $15^\circ$ .

The present model can explain the wakefield emission observed in our earlier 2D simulations when a laser pulse is incident normally on a nonuniform plasma slab [9]. In this case, because of the finite beam diameter, the excited plasma wave has a transverse wave vector, equivalent to the oblique incidence of many plane laser pulses. For a laser pulse profile  $a_L^2 = a_0^2 f_1(x - ct) f_2(y)$ , one can obtain an angular factor for the emission  $S_W(\theta, \tilde{\omega}) = k_{p0} \tilde{\omega} \tilde{f}_2(k_{p0} \tilde{\omega} \tan \theta) / \cos^2 \theta$ . Here  $\tilde{f}_2(k_y)$  is the Fourier transform of  $f_2(y)$ . More detailed discussions will be given elsewhere.

Finally, the present theory may partially explain the earlier experimental observations of THz emission by

Hamster *et al.* [7]. For example, mode conversion can explain their solid target data, where emission was observed in the direction of specular reflection with  $p$  polarization. The so-called nonresonant excitation with solid targets can be attributed to the steep density profiles. On the other hand, Hamster *et al.* [7(b)] reported that, for the chamber gas target, the THz emission was peaked in the forward direction and no radiation was detected in the back direction. This emission is likely not from mode conversion, but from the transient current produced through ponderomotive plasma wave generation as also found in our earlier simulations [9].

In conclusion, a laser wakefield can emit electromagnetic pulses though linear mode conversion. Such electromagnetic pulses can be potentially a powerful THz source capable of affording field strengths of a few GV/m, suitable for THz nonlinear physics. It also provides a new diagnosis of laser wakefield amplitudes and even wave breaking in the context of wakefield accelerators.

We thank Professor K. Nishihara and Professor M. Hangyo for their interest in this work. This work was supported in part by the JSPS-CAS Core-University Program on Plasma and Nuclear Fusion. Z.M.S. and J.Z. were also supported by the China NNSF (Grants No. 10390160, No. 10335020, and No. 10425416), the National High-Tech ICF Committee in China, the NKBRSF under Grant No. G1999075200, and the Knowledge Innovation Program, CAS.

- 
- [1] P. Sprangle *et al.*, Phys. Rev. Lett. **64**, 2011 (1990).
  - [2] T. Tajima and J.M. Dawson, Phys. Rev. Lett. **43**, 267 (1979).
  - [3] E. Esarey *et al.*, IEEE Trans. Plasma Sci. **24**, 252 (1996).
  - [4] S.C. Wilks *et al.*, Phys. Rev. Lett. **62**, 2600 (1989).
  - [5] Z.-M. Sheng *et al.*, J. Opt. Soc. Am. B **10**, 122 (1993); Z.-M. Sheng *et al.*, Phys. Rev. E **62**, 7258 (2000).
  - [6] S.V. Bulanov *et al.*, Phys. Rev. Lett. **91**, 085001 (2003).
  - [7] (a) H. Hamster *et al.*, Phys. Rev. Lett. **71**, 2725 (1993); (b) Phys. Rev. E **49**, 671 (1994).
  - [8] X.-C. Zhang *et al.*, Appl. Phys. Lett. **56**, 1011 (1990); R. Kersting *et al.*, Phys. Rev. Lett. **79**, 3038 (1997); G.L. Carr *et al.*, Nature (London) **420**, 153 (2002); M. Abo-Bakr *et al.*, Phys. Rev. Lett. **90**, 094801 (2003); W.P. Leemans *et al.*, Phys. Rev. Lett. **91**, 074802 (2003); P. Sprangle *et al.*, Phys. Rev. E **69**, 066415 (2004), and references therein.
  - [9] Z.-M. Sheng *et al.*, Phys. Rev. E **69**, 025401(R) (2004).
  - [10] W.L. Kruer, *The Physics of Laser Plasma Interaction* (Addison-Wesley, New York, 1988).
  - [11] R.W. Means *et al.*, Phys. Fluids **24**, 2197 (1981).
  - [12] D.E. Hinkel-Lipsker *et al.*, Phys. Rev. Lett. **62**, 2680 (1989); Phys. Fluids B **4**, 559 (1992).
  - [13] R. Lichters *et al.*, Phys. Plasmas **3**, 3425 (1996).
  - [14] E. Abedo and J.R. Sanmartin, Plasma Phys. Controlled Fusion **29**, 419 (1987).